

Characterization and Responsivity of Graphene Loaded Zinc Sulfide within Visible Light Spectrum

Sabreen A. Khalaf¹, Iftikhar M. Ali²

¹ Dept. of phys., College of science, Baghdad University.
sabreenali850@yahoo.com

² Dept. of phys., College of science, Baghdad University.
iftikhariq@scbaghdad.edu.iq

Abstract

Nanocrystal-ZnS-loaded graphene was synthesized by a facile co-precipitation route. The effect of graphene on the characterization of ZnS has been investigated. XRD results reveal that ZnS has cubic system while hexagonal structure has been observed by loading graphene during preparation ZnS. EDS analysis proves the presence of all expected elements in the prepared materials. Nanosize of fabricated materials has been measured using SEM technique. Also, it is found that the graphene plays a critical role to lowering optical energy gap of ZnS nanoparticles from 4 eV to 3.2 eV. The characterization of detector fabricated from these materials showed that the ZnS/graphene nanostructure exhibits color tunable to green region compared to bare ZnS which has responsivity at blue region due to introducing graphene.

Keywords: ZnS, graphene, nanocrystals, composites, detectors.

1. Introduction

Almost all materials system including metal, insulators and semiconductors show size dependent electronic or optical properties in the quantum size regime. Among these, the modification in the energy band gap of semiconductors is the most attractive one because of the fundamental as well as technological importance [1]. Semiconductors with widely tunable energy band gap are considered to be the materials for next generation flat panel displays, photovoltaic, optoelectronic devices, laser, sensors, photonic band gap devices, etc.

Zinc sulfide (ZnS) was one of the first semiconductors discovered and is also an important semiconductor material with direct wide band gaps for cubic and hexagonal phases of 3.72 and 3.77 eV, respectively. It has a high absorption coefficient in the visible range of the optical spectrum and reasonably good electrical properties. These ZnS semiconductor materials have a wide range of applications in electroluminescence devices, phosphors, light emitting displays, and optical sensors[2-6].

A single layer of graphene is called graphene nanosheet (GNS), which has a wide range of unique physical features, as well as its 2-dimensional planar structure, zero band gap, half metallicity and high electron mobility. All these electronic properties of the GNS and structural make it a promising route to use it in various applications, such as nanoelectronics, solid-state sensors, and spintronic [7-10].

Photoconductivity (PC) is defined as electrical conductivity resulting from photo-induced electron excitations in which light is absorbed. In semiconductors, photoconductivity arises due to interaction of photons with bound electrons of lattice atoms that leads to photo-generation of electron-hole pairs after absorption of photons which increases carrier density and conductivity of material [11,12]. Extensive study of photoconductivity has been made in nanoparticles, thin film, nanorods, nanowires and mixed lattice for different parameters [13,14].

In this work, the characterization of ZnS and ZnS/Gr has been revealed also, the effect of graphene nanosheet on the responsivity of zinc sulfide has been studied.

2. Experimental Details

ZnS nanoparticles were synthesized by co-precipitation chemical method. In a typical way to approach stoichiometric structure for zinc sulfide, a stock solution of Zn^{2+} was prepared by adding 0.1 M of $Zn(NO_3)_2 \cdot 6H_2O$ into 50mL of distilled water. A stock solution of S^{2-} was prepared by adding 0.2 M of Na_2S into 50mL of distilled water. Then put the first solution on magnetic stirrer at temperature of $80^\circ C$ for 1 hr, then the second solution is added drop wise and the whole solution is stirred for 30 min then filtered and washed several times using distilled water, ethanol and finally by acetone then dried using oven at $100^\circ C$ for 5 hr. For preparing ZnS/graphene, 0.1 g of graphene nanosheets which was purchased from sigma Aldrich is weighted and stirred with DMF solution for 6 hr then sonicated for another 6 hr to get homogeneous suspension. A appropriate volume of Gr suspension was added to stock solution of Zn^{2+} and stirred together at $80^\circ C$ for 1 hr and the same procedure was done. The resultant powders were characterized by XRD, EDS and SEM analysis. Thin films are prepared by spin coating technique. For thin films preparation, 10 mg from the powder of ZnS or ZnS/Gr was dissolved in 10 ml of distilled water and left it overnight for well dissolved and sonicated in ultrasonic bath for 30 min before spin coating process. Finally, the solution was spin-coated on substrates by a spin coater at a speed of 2000 rpm and repeated 5 times to obtain a homogeneous thin film and required thickness. The substrate was placed in oven at $100^\circ C$ for 5 min between each coating cycle.

3. Result and Discussion

3.1 Structural properties

3.1.1 XRD Analysis Results

Figure -1 shows the x-ray diffraction of ZnS and ZnS/Gr nanostructures. From figure (1a) it has been observed that pure ZnS has cubic zinc blende structure (pointed by * label) with comparison to the standard card ICDDPS (96-110-1051). The three main peaks of ZnS are observed in the diffractogram at 2Θ equal 28.3549, 47.5354, 56.195 corresponds to (111), (220) and (311) planes respectively. After addition of Gr to ZnS as shown in Fig. (1b), new phase for ZnS appeared that is hexagonal structure (pointed by # label) with comparison to the standard card ASTM (12-688) because Gr sheet has Hexagon structure (honeycomb lattice), so the graphene sheet becomes as a template to ZnS growth on this sheet. In the same time, graphene peaks appeared at 2Θ equal 26.6351, 62.6492, 67.7479 corresponds to (002), (227), (416,228) planes respectively (pointed by @ label).

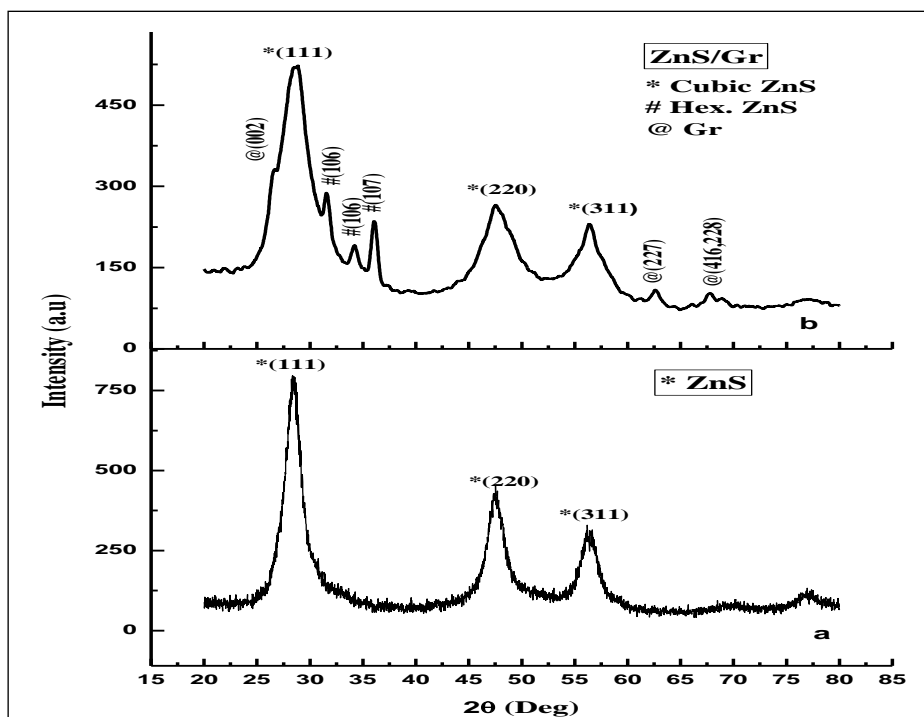


Figure-1 XRD patterns for ZnS and ZnS/Gr

The average crystallite size is calculated from Scherer formula [$D=0.9\lambda/(\beta \cos\theta)$] where λ is the X-ray wavelength (here $\lambda = 1.54060 \text{ \AA}$), θ is the Bragg angle and β is the full-width at half-maximum (FWHM) measured in radian.

Table-1 Structural Parameters of ZnS and ZnS/Gr which are diffraction angle, (hkl), d-spacing and FWHM.

Sample	2 θ (deg)	FWHM (Rad)	Plane (hkl)	D Crystallite size	Phase	Card no.
ZnS	28.3549	0.043611	111	3.281995	Cubic	96-110-1051
	47.5354	0.034889	220	4.34635	Cubic	5-0566
	56.195	0.027911	311	5.636229	Cubic	96-110-1051
ZnS/Gr	26.6351	0.024422	002	5.839009	Gr	23-64
	28.6179	0.052333	111	2.736683	cubic	96-110-1051
	31.5314	0.020933	106	6.916823	Hex	I2-688
	34.1819	0.024422	106	5.944541	Hex	I2-688
	36.0635	0.017444	107	8.36634	Hex	I2-688
	47.5354	0.069778	220	2.173182	Cubic	5-0566
	56.3367	0.055822	311	2.820021	Cubic	96-110-1051
	62.6492	0.022678	227	7.163442	Gr	22-1069

	67.7479	0.017444	416,228	7.973054	Gr	22-1069
--	---------	----------	---------	----------	----	---------

3.1.2 EDS Analysis Results

The chemical composition of pure ZnS and ZnS/Gr is shown in figure (2a and b). Table (2) illustrates EDS results and shows the weight and atomic percentage of Zn, S and C. The Zn and S peaks depict the characteristic chemical composition of the synthesized nanomaterials. The results reveal that after Gr addition the weight and atomic percentages of Zn and S reduce and increase for element C that prove the formation of ZnS/ graphene system.

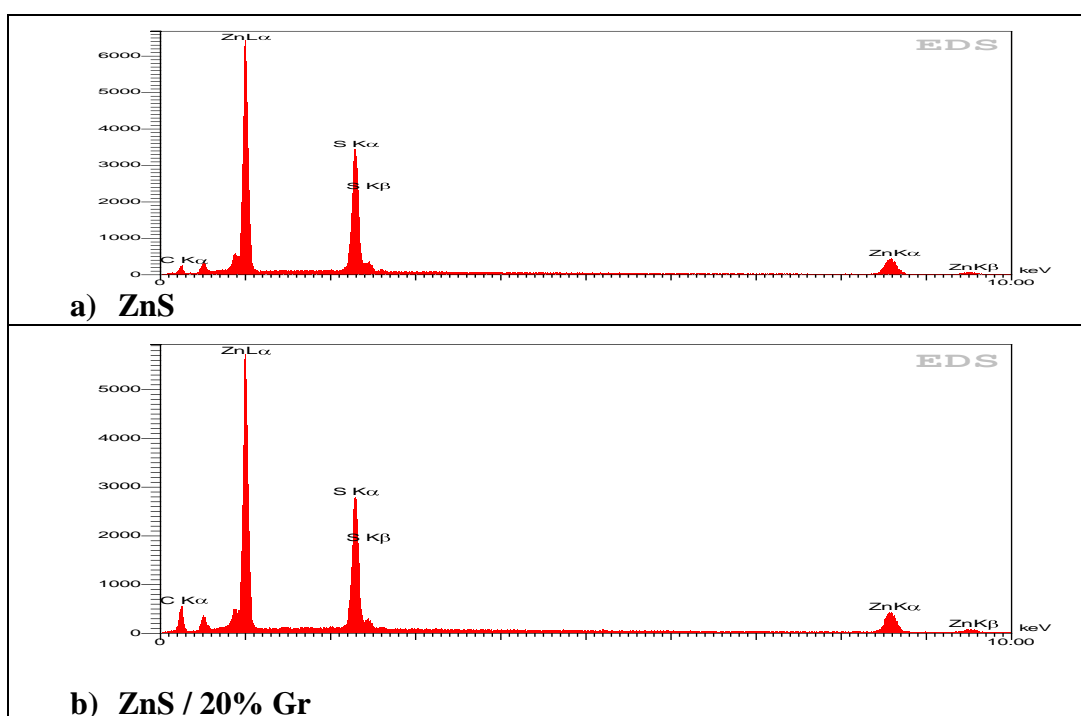


Figure (2) EDS analysis for ZnS and ZnS/Gr

Table (2) EDS measurements of ZnS/Gr system.

Sample	Elements	Weight %	Atomic %	Series
ZnS	S	22.84	22.26	K α
	Zn	57.92	27.69	K α
ZnS/Gr	C	32.02	67.15	K α
	S	16.63	13.06	K α
	Zn	51.36	19.79	K α

3.1.3 SEM Analysis Results

Scanning electron microscopy (SEM) is a versatile technique for studying morphology of materials. Figures (3a and b) illustrate the images of pure ZnS prepared by co-precipitation route without adding the graphene which has nanosize with nanoparticle structure where ZnS nanoparticles tend to aggregate without the dispersion of graphene. For ZnS/Gr, the interaction between the graphene and Zn^{2+} may be responsible for the uniform dispersion of ZnS nanoparticles on graphene and it is clear that ZnS nanoparticles are loaded on graphene nanosheet as shown in Figures (3c and d).

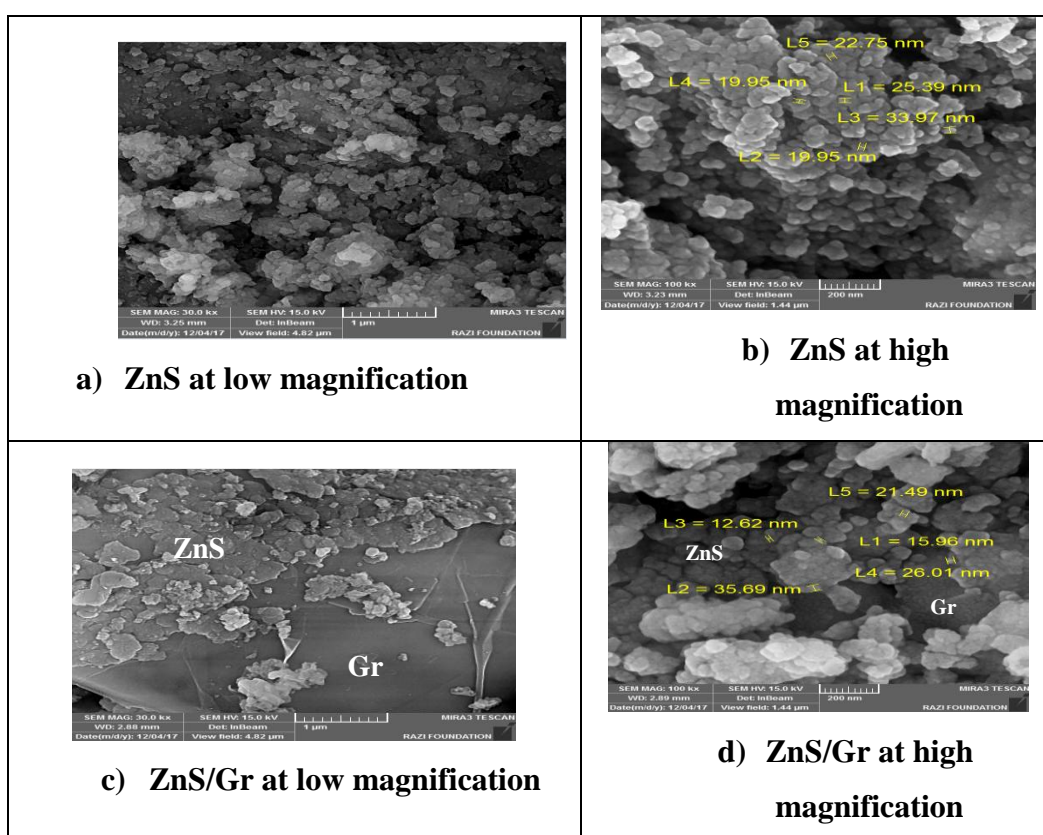


Figure (3) SEM images of ZnS and ZnS/Gr.

3.2 Electrical properties

3.2.1 I-V Characteristics for ZnS and ZnS/Gr

To investigate the type of electrical contact, I–V characteristics are taken for **ZnS and ZnS/Gr** and show a non-linear behavior this indicates that the electrical contact is not ohmic as shown in figure (4). I-V curve for ZnS has rectifier behavior because the reverse current is still constant with small value which equals to saturated current I_s and its rectifier factor which calculated by the relation [$rf = I_f/I_r$] is ~ 30 , which approaches ideal rectifier diode.

For ZnS/Gr, the carriers transported easily because there is lower rectification than that for pure ZnS as in figure (4).

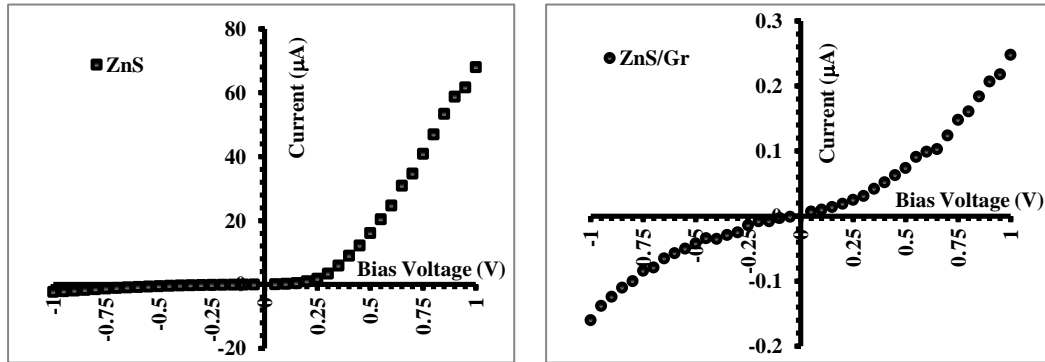


Figure (4): I-V characteristics in the dark for ZnS and ZnS/Gr.

In general the forward dark current is generated due to the flow of majority carriers and the applied voltage injects majority carriers which lead to decrease the value of built-in potential and decrease the width of the depletion layer. Then the majority and minority carrier concentration are higher than the intrinsic carrier concentration ($n_i^2 < n_p$) which leads to generate recombination current at the low voltage region (0-0.3 V) because that the excitation electrons from V.B to C.B will recombine with the holes which found at the V.B and this is observed by little increase in recombination current at low voltage region. The tunneling current has been represented at the high voltage region ($>0.3V$) where there is a fast exponential increase in the current magnitude with increasing the voltage and this is called diffusion current. Also the reverse bias current which also contains two regions, in the first region (low voltages $<0.3V$) the current slightly increases with increasing the applied voltage, and the generation current dominates, while at the high voltage region ($>0.3V$), the diffusion current dominates [15]. The value of saturation current I_s and ideality factor n are calculated from this equation $[n = (q/k_B T) (V / \ln(I_f / I_s))]$ where V and I_f are the forward bias voltage and forward current respectively, q is electronic charge, k_B is Boltzman constant and T is temperature which is 300K.

In forward bias, minority carriers are injected into quasi-neutral regions and these injected minority carriers recombine at surface. In reverse bias, minority carriers are extracted from quasi-neutral regions where extracted minority carriers are generated at surface.

From current-voltage measurements one can determine the potential barrier height (Φ_{Bn}) which can be determined by the relation $[\Phi_{Bn} = (k_B T / q) \ln(A A^* T^2 / I_s)]$ where A is the Schottky contact area which is 0.1485 cm^2 , A^* is the effective Richardson constant and I_s , n , Φ_{Bn} values are tabulated in Table (3):

Table (3): I_s , n and Φ_{β} for p-PS at different etching current densities in dark .

Sample	n	Φ_{β} (eV)	I_s (μA)
--------	-----	---------------------	-------------------------

ZnS	2.80	0.4377	1.79
ZnS/Gr	4.40	0.5540	0.02

3.2.2 Responsivity R_λ for ZnS and ZnS/Gr

The light responsivity of the detector is measured in the wavelength range of (200–900) nm under zero bias voltage. Figures (5) show the measured maximum values of responsivity and their values are in the UV region at 300 nm which is for ZnS excitonic transition and the other is at 490 nm which is corresponding to transition of electrons between zinc vacancy acceptor level and sulfur vacancy donor level and this observation is agree with Huaming *et al.* [15].

After graphene loading, there is red shift for these two peaks maxima which are at 320 nm for UV region and 510 nm for visible region. So, one can tune ZnS nanoparticles by functionalization with graphene nanosheet. Also, there is broad peak that means the material has response for wide range of wavelength.

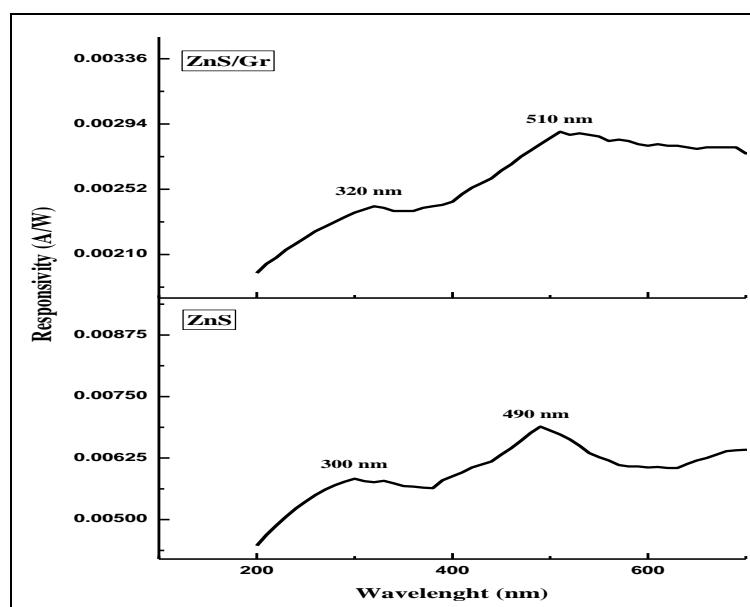


Figure (5): The variation of spectral responsivity of ZnS and ZnS/Gr as a function of the wavelength.

Table (4): The values of spectral responsivity corresponding to maximum wavelength for ZnS and ZnS/Gr

Sample	Wavelength (nm)		Responsivity (A/W)	
ZnS	300	490	0.00583	0.00689
ZnS/Gr	320	510	0.00241	0.00289

4. Conclusions

ZnS/graphene nanostructure has been synthesized by a simple co-precipitation route. The ZnS nanoparticles with a size below 100 nm are uniformly loaded on the graphene sheets when using Zn^{2+} as the precursor. The ZnS/graphene nanostructure exhibits improved optical and electrical properties compared to bare ZnS due to the incorporation of graphene which acts both as a buffer to alleviate the volume changes and as a separator to refrain the aggregating of the particles. Furthermore, the introduced graphene offers a conducting channel for ZnS and increases the specific surface area, enhancing the detecting visible wavelengths.

References

- [1] R. Rossetti, J.L. Ellison, J.M. Gibson, L.E. Brus, *J. Chem. Phys.* **80**, (1984) 4464.
- [2] K. Jayanthi, S. Chawla, H. Chander, and D. Haranath, Structural, optical and photoluminescence properties of ZnS: Cu nanoparticle thin films as a function of dopant concentration and quantum confinement effect, *Cryst. Res. Technol.* V.42 (10) (2007) pp. 976 – 982).
- [3] T. Ben Nasr, N. Kamoun , M. Kanzari, R. Bennaceur, Effect of pH on the properties of ZnS thin films grown by chemical bath deposition, *Thin Solid Films*, V. 500, (2006) pp.4-8.
- [4] B.L.Sharma, R.K.Purohit, "Semiconductors Heterojunctions", Academic Prees, Inc, Oxford, NewYork (1974)pp.1-15.
- [5] G.Milnes & D.L.Feucht, " Heterojunctions and Metal Semiconductors Junctions"Academic Prees, London (1972).
- [6] Huang Jian, Wang Lin-Jun, Tang Ke, Xu Run, Zang Ji-Jun, Lu Xiong-Gang, Xia Yiben, Photoresponse Properties of an n-ZnS/p-Si Heterojunction, *Chin. Phys. Lett.* V. 28, N. 12 (2011) 127301-3.
- [7] A. K. Geim and K. S. Novoselov, "The rise of graphene," *Nature materials*, vol. 6, pp. 183- 191, 2007.
- [8] L. Ponomarenko, F. Schedin, M. Katsnelson, R. Yang, E. Hill, K. Novoselov, *et al.*, "Chaotic Dirac billiard in graphene quantum dots," *Science*, vol. 320, pp. 356-358, 2008.
- [9] F. Schedin, A. Geim, S. Morozov, E. Hill, P. Blake, M. Katsnelson, *et al.*, "Detection of individual gas molecules adsorbed on graphene," *Nature materials*, vol. 6, pp. 652-655, 2007.
- [10] Y. Zhou, J. Zhang, D. Zhang, C. Ye, and X. Miao, "Phosphorus-doping-induced rectifying behavior in armchair graphene nanoribbons devices," *Journal of Applied Physics*, vol. 115, p. 013705, 2014.

- [11] Callister J. and Malinowski S., “Optical Properties In Anderson”, *Materials Science and Engineering: An Introduction* (6th). John Wiley & Sons, Inc.: New Jersey, 707–729 (2003).
- [12] Mishra S. K., Srivastava R. K., Prakash S. G., Yadav R. S. and Panday A. C., “Photoluminescence and photoconductive characteristics of hydrothermally synthesized ZnO nanoparticles”, *Opto–Electronics Rev.*, 18, 467 (2010).
- [13] Eman M. N., “Fabrication and Characterization of n-ZnS/p-Si and n-ZnS:Al/p-Si Heterojunction”, *Int. J. Engineering and Advanced Technology*, 3(2) (2013).
- [14] Law J. B. and Thong J. T., “Simple fabrication of a ZnO nanowire photodetector with a fast photoresponse time”, *Appl. Phys. Lett.*, 88, 133114 (2006).
- [15] Huaming Y., Chenghuan H., Xiaohui S. and Aidong T., “Microwave-assisted synthesis and luminescent properties of pure and doped ZnS nanoparticles”, *J. of Alloys and Compounds*, 402, 274–277 (2005).